Materials Science Forum Vols. 794-796 (2014) pp 130-136

doi:10.4028/www.scientific.net/MSF.794-796.130

Modification of eutectic Si in Al-Si based alloys

J.H. Li[1, a *], M. Albu[2, b], T.H. Ludwig[3, c], Y. Matsubara[4, d], F. Hofer[2, e],

L. Arnberg[3, f], Y. Tsunekawa[4, g], P. Schumacher[1,5, h]

[1] Chair of Casting Research, University of Leoben, Franz-Josef Str.18, A8700 Leoben, Austria
[2] Institute for Electron Microscopy and Nanoanalysis (FELMI), Graz University of Technology, Center for Electron Microscopy Graz, Steyrergasse 17, A-8100 Graz, Austria
[3] Department of Materials Science and Engineering, Norwegian University of Science and Technology, N-7491 Trondheim, Norway
[4] Toyota Technological Institute, Hisakata 2-12-1, Tempaku, Nagoya 468-8511, Japan
[5] Austrian Foundry Research Institute, Park Str.18, A8700 Leoben, Austria

[a] jie-hua.li@hotmail.com, [b] mihaela.albu@felmi-zfe.at, [c] thomas.ludwig@material.ntnu.no,

[d] tsunekawa@toyota-ti.ac.jp, [e] ferdinand.hofer@felmi-zfe.at, [f] lars.arnberg@ntnu.no,

[g] tsunekawa@toyota-ti.ac.jp, [h] peter.schumacher@unileoben.ac.at

Keywords: Al-Si alloy; Modification, Eutectic solidification; TEM

Abstract. The paper provides a new insight into the modification of eutectic Si in Al-Si based alloys. To date, impurity-induced twinning mechanism and twin plane re-entrant edge mechanism are the well-accepted theories. However, neither IIT nor TPRE can be used to interpret all modification observations. Therefore, a re-consideration of modification mechanisms is still required. In this contribution, recent advances on the understanding the modification of eutectic Si are reviewed. Two different cases are highlighted. In the case of Sr, Na and Eu addition, eutectic Si was modified from a faceted to a fibrous morphology, which involves the formation of multiple Si twinning. In the case of Yb and Ca addition, eutectic Si was refined to a smaller size, but still maintained a plate-like morphology. The possible modification mechanism was thus discussed in terms of (i) adsorption of atoms at twin re-entrant edge, and (ii) segregation across $\{111\}_{Si}$ growth planes. Furthermore, solute entrainment of modifying elements (M) was introduced to interpret the formation of Al_2Si_2M phase or M-rich clusters within Si crystals.

Introduction

Modification of eutectic Si in Al-Si alloys can be dated back to 1920 [1], since the first modification phenomenon was discovered by Pacz. Recent technological developments of electron microscopy, e.g. high resolution transmission electron microscopy and atom probe microscopy, make it possible to investigate the modification mechanisms at an atomic scale. To date, it is generally accepted that the impurity-induced twinning (IIT) [2] and the twin plane re-entrant edge (TPRE) growth mechanism [3, 4] are valid under contain conditions. The IIT mechanism postulates that the impurities (i.e. Sr, Na) are adsorbed on the growing surfaces of Si producing frequent twinning. The TPRE mechanism proposes that Si growth occurs more readily at the re-entrant edge. However, neither IIT nor TPRE can be used to interpret all the modification observations, i.e. the Yb additions into Al-Si alloys only refine, rather than modify, the eutectic Si [5], even though Yb has an exactly suitable radius ratio ($r_{Yb}/r_{Si} = 1.646$) according to the IIT mechanism. A similar investigation on the effects of rare earth elements addition, has been also reported [6]. Only Eu modified the eutectic Si to a fibrous morphology, while other remaining rare earth elements (i.e. La, Ce, Pr, Nd, Sm, Gd, Tb, Dy, Ho, Er, Tm, Yb and Lu) solely refine the plate-like Si, although all these elements have a similar radius ratio, which is expected to modify Si according to the IIT mechanism. The observed disagreements strongly indicate that the well-accepted IIT, based on atomic radius alone, is not capable of explaining modification, and additional mechanisms are still required. A revision of the

factors influencing the modification of eutectic Si is thus of great necessity in order to elucidate this important melt treatment for Al-Si based alloys.
In this paper, we report TEM observations of Si twinning in a series of Al-5 wt.% Si alloys with Sr, Na, Eu, Ca or Yb additions, with a special focus on the distribution of modifier elements within the Si crystals. The factors affecting the modification of eutectic Si are also discussed, with the aim to revise the well-accepted modification mechanisms and to interpret the different observations in the cases of different modifier elements.

Experimental material and procedures

A series of Al-5 wt. % Si alloys (wt. %, used throughout the paper, unless specified noted) each with a trace addition of 200 ppm Sr, 50 ppm Na, 500 ppm Eu, 250 ppm Ca and 6100 ppm Yb were prepared by using arc melting and subsequent melt spinning. The details on sample preparation (i.e. arc melting and melt spinning) have been reported in [7].
It is noteworthy that Na (50 ppm) was added by Al-5Si-200 ppm Na master alloy manufactured from 5N (99.998) Al, 5N Si and 2N Na. The Al-5Si-200 ppm Na master alloy was produced using conventional die casting under protection of Ar. Eu (500 ppm) was added by Al-5Si-2Eu master alloy manufactured from 5N Al, 5N Si and 2N Eu. The Al-5Si-2Eu master alloy was produced using conventional die casting under protection of Ar. Sr (200 ppm), Ca (250 ppm) and Yb (6100 ppm) additions were made by using Al-4Sr, Al-10Ca, Al-5Yb master alloys produced from 5N Al, 2N Sr; 5N Al, 2N Ca; and 5N Al, 2N Yb, respectively.
The ribbons for TEM investigations were mechanically ground, polished and dimpled to about 30 μm, and then ion-beam milled using a Gatan Precision Ion Polishing System (PIPS, Gatan model 691). A constant preparation temperature (about -10 ºC) was maintained by using a cold stage during ion beam polishing. TEM was performed using a Philips CM12 microscope operated at 120 kV. High resolution TEM micrographs and the EDX investigations were performed using a Cs-corrected JEOL-2100F microscope operated at 200 kV. The high resolution STEM micrographs and the EDX investigations were performed using a monochromated and probe corrected FEI Titan^{3TM} G2 60-300 (S/TEM) microscope operated at 300 kV using an X-FEG high brightness emission gun. The high resolution images in STEM mode were recorded with a beam diameter of 0.1 nm and 0.039 nA current using the high angle annular (HAADF) and dark field (DF) detectors. X-ray spectra have been acquired by the SuperX detection system (ChemiSTEM^{TM} technology) with a 120 mm acquisition area which reduces significantly the acquisition times. Elemental quantification of the EDX spectra was performed using the Zeta factor method [8]. The images and spectra were recorded by a Gatan Digiscan unit and Digital Micrograph software, and have been corrected for dark current and gain variations.

Results

Fig. 1 shows a typical microstructure of a melt spun high purity Al-5Si alloy without any modifier addition. Some Si particles are distributed along the grain boundary (Fig. 1a). One Si particle was tilted to the principal twinning orientation of Si (<011>) (Fig. 1b). Viewed from $[011]_{Si}$ zone axis, the Si particle appears to be twinned (Fig. 1c), although the number density of Si twins appears to be low. It should be pointed out that Si twinning was grown along one special plane (i.e. $\{111\}_{Si}$), rather than multiply twinned, as shown in Fig. 2.
The addition of Sr (up to 200 ppm) to a melt spun Al-5Si alloy promotes Si twinning during solidification. In contrast to Fig. 1 (without Sr addition), most Si particles were multiply twinned. Fig. 2 shows a multiply twinned Si particle in melt spun Al-5Si-200 ppm Sr alloy. Fig. 2b shows the selected area diffraction pattern (SADP) taken by tilting to the $<011>_{Si}$ zone axis with double diffractions of two variants. Figs. 2c and d show the central dark field images taken from two different diffraction spots corresponding to two different variants, as marked in Fig. 2b.
Fig. 3a shows a low magnification HRSTEM-HAADF image of multiply twinned Si particles and Al_2Si_2Sr particle in melt spun Al-5Si-200 ppm Sr alloy. Fig. 3b was enlarged from one area as marked with a dashed line in Fig. 3a, showing a Al_2Si_2Sr particle at the grain boundary. The size of

the Al_2Si_2Sr particle is about 10 nm. Due to the high disregistry between the Si crystal and the Al_2Si_2Sr intermetallic, it is highly unlikely that Al_2Si_2Sr intermetallic acts as nuclei for Si [7]. Fig. 3c was enlarged from the other area as marked with a dashed box in Fig. 3a, showing a multiply twinned Si particle. As expected from the TPRE mechanism, Sr-rich clusters (Al-Si-Sr) were observed at the re-entrant edge (Fig. 3d) and along the Si twinning (Fig. 3e). Bright contrast in STEM-HAADF image corresponds to a higher Z (atom number) since the HAADF signal scales with Z^2 (Z_{Sr} is 38, much higher than Z_{Al} (13), Z_{Si} (14)). It should be noted that, for clarity, Al and Si peaks were not shown in the range of 7-16 keV. Only the peaks of Cu (about 8 keV) and Sr (about 14 keV) are highlighted (Fig. 3f). It should be also noted that the signal of Cu (at about 8 keV) originates from the Cu ring supporting the TEM sample. As described above, EDX analysis was performed using a beam diameter of 0.1 nm. The EDX analysis taken from the marked area (Fig.3d) indicates that Sr-rich clusters (Al-Si-Sr) are present at the re-entrant edge.

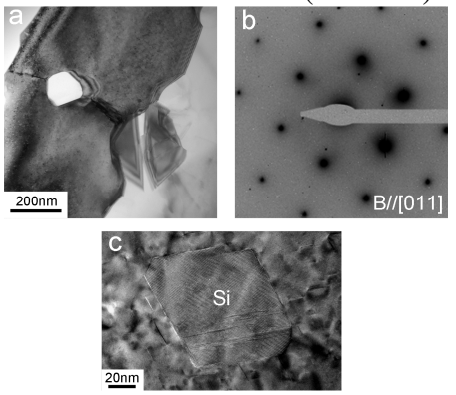

Fig. 1: (a) TEM bright field image, (b) corresponding selected area diffraction pattern, and (c) HRTEM image of Si particles in melt spun Al-5Si alloy.

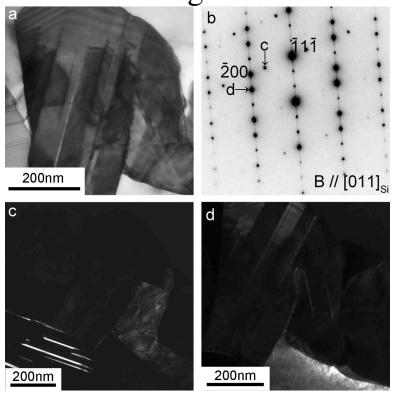

Fig. 2: (a) TEM bright field image, (b) corresponding [011] SADP, (c), (d) dark field images using the diffraction spots as marked in (b), in melt-spun Al-5Si-200 ppm Sr alloy.

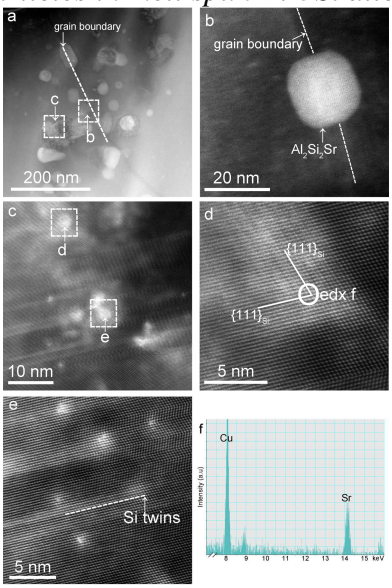

Fig. 3: (a-e) STEM-HAADF images in melt-spun Al-5Si-200 ppm Sr alloy, (f) EDX analysis of the Sr-rich cluster, as marked in (c).

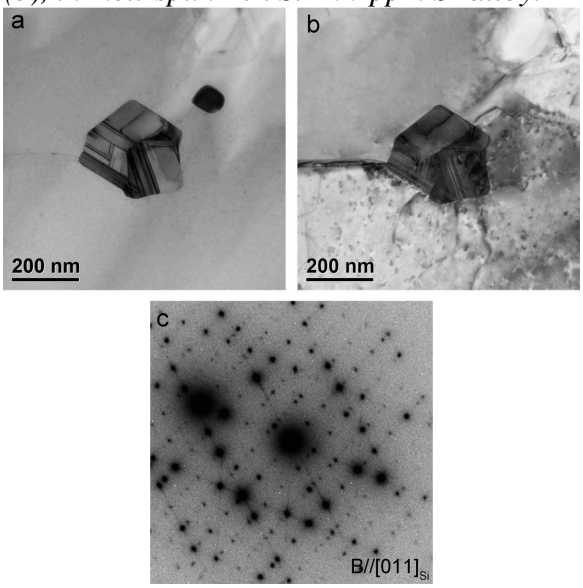

Fig. 4: (a) (b) TEM bright field images, (c) corresponding [011] SADP, of a Si particle, in melt-spun Al-5Si-50 ppm Na alloy.

The addition of Na (up to 50 ppm) to a melt spun Al-5Si alloy also promotes a significant increase of Si twinning, as shown in Fig. 4. After tilting to the principal twinning orientation of Si (<011>), the number density of Si twins (Fig. 4b) appears to be much higher compared with the Al-5Si alloys without (Fig. 1c) and with (Fig. 2a) 200 ppm Sr addition. It should be noted that no attempt was made to take STEM-HAADF image from the Na modified alloy, because the atom numbers of Al,

Si and Na are very close (Z_{Na} = 11). The brightness contrast of Na is significantly weaker than that of Sr (Z_{Sr} = 38).

The addition of Eu (up to 500 ppm) to a melt spun Al-5Si alloy also results in a significant increase of Si twinning, as shown in Figs. 5. Higher cooling rates during melt spinning induce the dispersion of Si into the Al matrix. No Si particle was observed in melt spun condition. However, after DSC heating, multiply twinned Si particles were observed. Furthermore, Eu-rich clusters (Al-Si-Eu) were measured at the re-entrant edge (Fig 5d). Eu could not be measured at any other defect free region or away from re-entrant edge. This result is fully consistent with the case of Sr and / or Na addition.

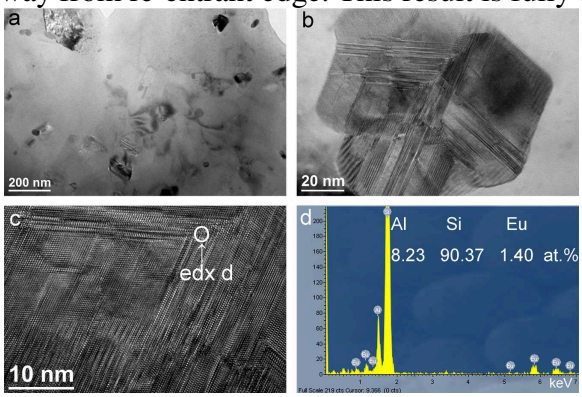

Fig. 5: TEM bright field image (a), high resolution TEM images (b), (c) and EDX analysis (d) of the Si particle in Al-5Si-500 ppm Eu after DSC cooling from 600 °C to 400 °C with a rate of 10 °C/min.

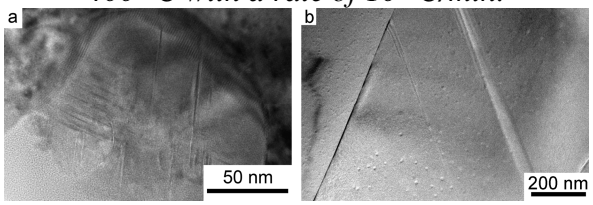

Fig. 7: TEM bright field images taken from Al-5Si-250 ppm Ca alloy in melt spun condition(a) and after DSC heating (b).

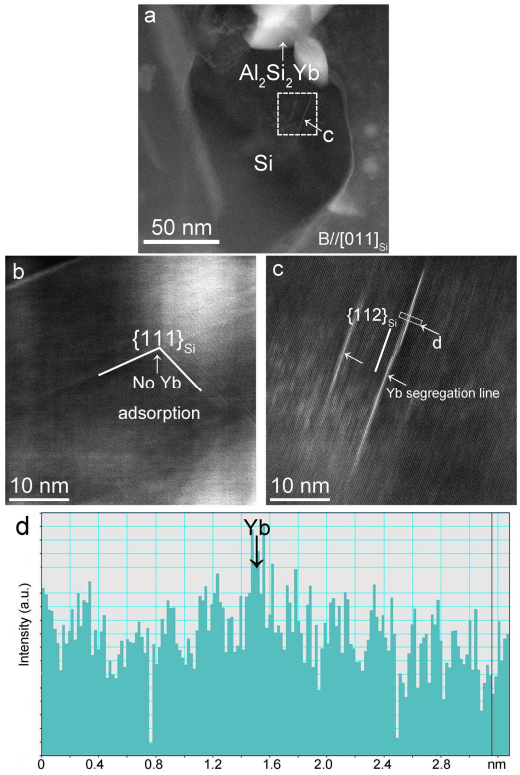

Fig. 6: (a-c) STEM-HAADF images in melt-spun Al-5Si-6100 ppm Yb alloy. (d) shows the intensity across the line in (c).

The addition of Yb (up to 6100 ppm) to a melt spun Al-5Si alloy has no significant effects on the Si twinning, when compared with the addition of Sr (up to 200 ppm) (Fig. 2a), Na (up to 50 ppm) (Fig. 4), and Eu (up to 500 ppm) (Fig. 5). Fig. 6 shows a faceted Si crystal on the grain boundary in melt spun Al-5Si-6100 ppm Yb alloy. The Si particle was also tilted to the principal twinning orientation of Si (<011>$_{Si}$), however, no significant Si twinning was observed, even in melt spun condition. A similar observation has also been reported for conventional casting conditions [5]. This observation is in contrast to the prediction of the IIT and the TPRE mechanism, highlighting the importance of the adsorption of modifying elements. Furthermore, no adsorption of Yb was observed at the re-entrant edges (Fig. 6b). When the sample was tilted away from <011>$_{Si}$ (about 30 °) (Fig. 6c), two Yb-rich segregation lines were observed along the {111}$_{Si}$ growth plane (Figs. 6c,d). These Yb-rich segregation lines can be attributed to the solute entrainment during Si growth. The Al_2Si_2Yb phase was also observed in the vicinity of the Si particle (Fig. 6a). However, similar to the β-Al_5FeSi and Al_2Si_2Sr phases, the Al_2Si_2Yb phase was not regarded as an effective nucleation site for eutectic Si due to its large disregistry between the Si crystal and Al_2Si_2Yb intermetallic.

In contrast to the Yb addition, the addition of Ca (up to 250 ppm) to a melt spun Al-5Si alloy also has a notable effect on the Si twinning. Fig. 7a shows a representative Si particle in melt-spun Al-5Si-250 ppm Ca alloy. Viewed from the [011] $_{Si}$ zone axis, the Si particle appears to be multiply twinned. This observation is in contrast to the previous reports on melt spun Al-5Si alloys without trace element additions (Fig. 1), where most Si twins were grown along one special plane (i.e. {111} $_{Si}$), rather than multiply twinned. This indicates that the presence of Ca promotes a significant

Si twinning in the presence of high cooling rates. However, it should be noted that the observed multiply twinned Si can be attributed to (i) higher cooling rates during melt spinning, and (ii) the insufficient time for adsorbed Ca atoms to be segregated away from the Si interface.
Fig. 7b shows a representative low magnification image of a larger Si particle after DSC heating. The Si crystal appears to have a plate-like morphology. Again, Si twinning was observed, although the number density of twins was reduced compared to the Si twinning in melt-spun condition. More importantly, most Si twinning was grown with a special $\{111\}_{Si}$, rather than being multiple twinned. This is in contrast to the case of Sr and Na addition, where highly multiple twinned Si is present even after DSC heating.

Discussion

The cases of Sr, Na and Eu additions will be discussed for the Sr addition, due to a lack of a direct observation of Na and Eu in the STEM images. However, it should be pointed out that a similar behaviour can be expected for Sr, Na and Eu on the basis of our above observations. For clarity, Fig. 8 shows a schematic representation of the Sr solute transport and entrainment ahead of the solidification front of eutectic Si in Al-Si alloys.
In the liquid state, the alloying elements (i.e. Al, Sr and Si) are randomly distributed, although solute clustering (i.e. Si clustering) may occur [9]. The micro-segregation of Si atoms in the melt at high temperatures has been reported in an Al-16Si alloy using θ- θ high temperature X-ray diffraction, rapid solidification, vertical centrifugal casting, and DSC [9]. During the growth of the Si crystal (Fig. 8a), Sr and Al solute will segregate ahead of the solidification front ($k_{Al} < 1$ and $k_{Sr} < 1$). A redistribution of Sr and Al, and thus an enrichment of Sr ahead of the solidification front of Si may occur. During the continuous growth of the Si crystal, adsorption of Sr on the $\{111\}_{Si}$ plane occurs at the re-entrant edge (Fig. 8b). According to the IIT mechanism, the adsorption of Sr promotes the formation of multiple Si twinning. The same also holds for the further Si growth along the newly created $\{111\}_{Si}$ planes. The adsorption of Sr on the $\{111\}_{Si}$ growth planes may also yield further re-entrant edges (Fig. 8c). In this case, Si growth will start from another $\{111\}_{Si}$ plane. Similarly, an enrichment of Sr in a local area and multiple Si twinning occurs. Finally, once the $\{111\}_{Si}$ planes fold on each other, the solute entrainment of the segregation fields occurs (Fig. 8d). On subsequent cooling, the solute entrainment of Al and Sr within the Si matrix forms Sr-rich particles with a different morphology and composition (mostly likely Al_2Si_2Sr).
It should be pointed out that solute entrainment is different from solute trapping. Solute entrainment is caused by solute segregation of overlapping Si crystal growth in the solid, while, solute trapping freezes the solutes. Therefore, solute trapping can only occur at an extremely high cooling rate (i.e. after laser remelting). No complete solute trapping was observed in our case, even after melt spinning. This indicates that the cooling rates and/or undercooling is still not significantly high enough to trap solutes, and to result in a chemically partitionless (diffusionless) process. Thus, solute trapping was not taken into consideration here.
The proposed solute entrainment can be used readily to interpret the observation of Sr-rich clusters using APT. The observed Sr-rich clusters may be an artefact caused by solute entrainment, rather than a “true” modification mechanism. We propose that the adsorption of Sr on the $\{111\}_{Si}$ growth planes and at the twin re-entrant edges is the dominant factor for the modification of eutectic Si in Al-Si alloys. It is the adsorption of Sr that leads to roughening and the formation of extended pits and regrowth structure, and causes multiple Si twinning [10].

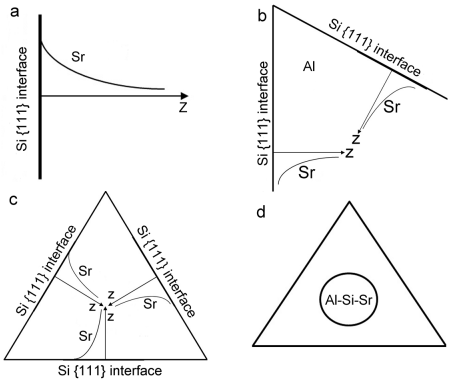

Fig. 8: Schematic representation of Sr solute entrainment, forming Sr-rich clusters.

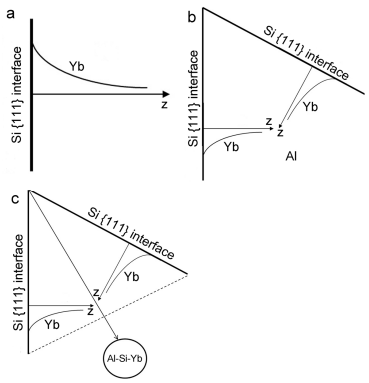

Fig. 9: Schematic representation of Yb segregation and Yb solute entrainment.

In contrast to Sr, Na and Eu additions, no significant multiple Si twinning was observed in the case of Yb and Ca additions (after DSC heating). Only a refinement, rather than a modification of the eutectic Si was observed [5]. For clarity, Fig. 9 also shows a schematic representation of the Yb segregation and entrainment of Yb solute in Al-Si alloys. Similar to the case of Sr addition (Fig. 8), in the liquid state, the alloying elements (i.e. Al, Yb and Si) were randomly distributed (Fig. 9a). During the growth of the Si crystal (Fig. 9a), Yb and Al solute will segregate ahead of the solidification front ($k_{Al} < 1$ and $k_{Yb} < 1$). A redistribution of Yb and Al, and thus an enrichment of Yb may occur. In contrast to Sr addition, the adsorption of Yb does not occur on $\{111\}_{Si}$ planes during continuous Si growth. Instead, Yb atoms diffuse out and are not present within Si. This hypothesis can be strongly supported with our observation (Fig. 6) and the previous report [11] that Yb is present just adjacent to the Si particle. No impurity induced twinning effect can be achieved because insufficient Yb atoms remained at the re-entrant edge. With the continuous Si growth, the solute entrainment (Fig. 9b, c) may occur along few twins, depending on the growth rate and local solute redistribution. If this kind of solute entrainment occurs, more and more Yb atoms will be entrained, forming a solute entrainment line (Fig. 9c), as observed in Fig.6c. However, it should be pointed out that although a series of atomic Yb-rich segregation lines form, no significant effects on the Si twinning can be expected because only an insufficient number of Yb atoms remained within the Si crystal. Due to the absence of Yb atoms at the re-entrant edge, Yb addition (up to 6100 ppm) does not promote the formation of the multiply Si twinning (Fig. 6), if any, only single Si twinning can be observed. Furthermore, no Al_2Si_2Yb particle was observed within Si. Instead, most Al_2Si_2Yb particles were observed adjacent the Si phase (Fig. 6a).

Conclusions

A revised modification mechanism was proposed. For the first time, the solute entrainment of the modifier element (M) was introduced to interpret the formation of Al_2Si_2M phases or M-rich clusters within Si crystals. More importantly, these kinds of Al_2Si_2M phases or M-rich clusters are proposed to be an artefact caused by solute entrainment during Si growth, rather than a "true" modification mechanism. The segregation of Yb along the $\{111\}_{Si}$ growth planes was also found to be different from the adsorption of Sr. The absence of Yb within the Si crystals, in particular at the twin re-entrant edges, leads to a refinement, rather than a modification of eutectic Si in Al-Si alloys. This proposed modification mechanism can be used to interpret the different observations in the cases of different modifying elements.

Acknowledgments

J.H. Li acknowledges Prof G. Dehm for granting access to the TEM facility at the Erich Schmidt Institute of Materials Science of the Austrian Academy of Sciences.

References

[1] A. Pacz U.S Patent No. 1387900; 1921.
[2] S.Z. Lu, A. Hellawell, Met. Trans. A 18(1987) 1721-1733.
[3] R.S. Wanger, Acta Metall. 8(1960) 57.
[4] R.D. Hamilton, R.G. Seidensticker, J. Appl. Phys. 31(1960) 1165.
[5] J.H. Li, S. Suetsugu, Y. Tsunekawa, P. Schumacher, Metall. Mater. Trans. A 44(2013) 669-681.
[6] K. Nogita, S.D. McDonald, A.K. Dahle, Mater. Trans. 45(2004) 323-326.
[7] J.H. Li, M. Zarif, G. Dehm, P. Schumacher, PHIL. Mag. 92(2012) 3789-3805.
[8] M. Watanabe, D.B. Williams, Journal of Microscopy. 221(2006) 89-109.
[9] W.M. Wang, X.F. Bian, J.Y. Qin, S.I. Syliusarenko, Metall. Mater. Trans. A 31(2000) 2000-2163.
[10] K.H. Wu, Y. Fujikawa, T. Nagao, Y. Hasegawa, K.S. Nakayama, Q.K. Xue, E.G. Wang, T. Briere, V. Kumar, Y. Kawazoe, S.B. Zhang, T. Sakurai, Physical Review Letters 91(2003) 126101.
[11] K. Nogita, H. Yasuda, M. Yoshiya, S.D. McDonald, K. Uesugi, A. Takeuchi, Y. Suzuki, J. Alloys Compd. 489(2010) 415-420.